Article:
Zainol, Z., Morrisset, D., Alapati, A.K. et al. (2026) Through-thickness fire-retardant distribution influence on fire retardancy properties of glass fibre powder epoxy composites. Results in Materials, 31. 100986. ISSN: 2590-048X

https://doi.org/10.1016/j.rinma.2026.100986

Results in Materials 31 (2026) 100986

Contents lists available at ScienceDirect

Results in Materials

journal homepage: www.sciencedirect.com/journal/results-in-materials

Through-thickness fire-retardant distribution influence on fire retardancy properties of glass fibre powder epoxy composites

Zalia Zainol [a,b], David Morrisset [b], Arun Kumar Alapati [a], Conchúr M. Ó Brádaigh [a], Rory M. Hadden [b], Colin Robert [a,*]

[a] Composite Group, School of Engineering, Institute for Materials and Processes, The University of Edinburgh, Edinburgh, EH9 3FB, UK
[b] Centre for Fire Safety Engineering, The University of Edinburgh, Edinburgh, EH9 3JL, UK

ARTICLE INFO

Keywords:
DOPO
Gradient
GFRP
Cone calorimeter

ABSTRACT

Despite advances in novel fire retardants, how they are incorporated into a flammable substrate and the impact of this on fire retardancy remains underexplored. This study investigates how different fire-retardant (FR) distribution modes affect the flammability of an epoxy-based glass fibre composite. Specifically, three distribution modes are examined: homogenous (i.e., evenly distributed FR across layers), gradient (i.e., controlled variation in-depth), and top (i.e., all FR concentrated in the top layer). The study also varied the volume fraction of DOPO (9,10-Dihydro-9-oxa-10-phosphaphenanthrene-10-oxide) in each plate to observe its effect on fire performance. Nine glass fibre reinforced polymer (GFRP) plates were manufactured with different distribution modes and DOPO volumes using a manual layup method. The fire performance of these plates was assessed using the cone calorimeter, analysing heat release rate (HRR), carbon monoxide (CO) generation and time to ignition (TTI). Results indicate that the gradient and top distribution modes are more effective in reducing the flammability with a lower total volume of DOPO compared to the homogeneous mode. Optimizing the distribution mode by mainly placing DOPO on the surface layer with a lower total volume is more effective than using a higher volume of DOPO distributed homogeneously. This research exemplifies how FR loadings can be modified to allow optimization of fire performance, material properties and cost.

1. Introduction

Due to its advantageous properties, including its excellent resistance to solvents and exceptional electrical insulation, epoxy resin is a highly sought-after thermosetting material in various industries [1–3]. However, epoxy resin is flammable and has a typical limiting oxygen index (LOI) of 19%, thus necessitating modification with fire retardants (FRs) for many applications [4]. Epoxy, an organic substance, is liable to combustion, making it vulnerable to fire [5]. Hence, researchers have explored various methods to reduce the flammability of epoxy-based composites, leading to the development of fire-retardant epoxy polymers (FREPs) [6–10]. It has been shown that adding compounds containing halogens [11,12], phosphorus [13,14], nitrogen [15–17], and silicon [18,19] to the epoxy matrix is an efficient approach to reduce their flammability.

Furthermore, fibre-reinforced epoxy composites have gained popularity as structural materials in various applications due to their remarkable mechanical strength, thermal stability, and high ratio of strength to weight [20]. Glass fibres are favoured among various fibre types for their high stiffness and low density [21]. In addition, glass fibres have a high tensile strength, with a range of 2.4 to 4.9 GPa and they are cost-effective [22–24]. There are many studies that focus on improving the fire performance of glass fibre-reinforced epoxy composites to increase their fire retardancy [25–27]. However, the flammability of epoxy-based glass fibre composites using powder epoxy modified with the inclusion of fire retardant as the polymer matrix has yet to be thoroughly investigated.

In various industries, including heavy-duty applications [28] and automated composite manufacturing [29], there's a growing demand for affordable carbon fiber composites suitable for a range of applications such as marine and automobiles. Powder-based epoxy has gained popularity as an alternative to liquid epoxy due to its superior properties [30–39], including a low thermal exothermic reaction [35,39] for faster manufacturing, enhanced thermal stability [39] compared to liquid

* Corresponding author.
E-mail address: c.robert@sheffield.ac.uk (C. Robert).

https://doi.org/10.1016/j.rinma.2026.100986
Received 28 April 2025; Received in revised form 22 January 2026; Accepted 13 June 2026
Available online 18 June 2026

epoxy, and low minimal viscosity [32] during melting, which improves fibre wetting and compatibility with FRs. One of the main reasons for this shift in preference is its sustainability. With no solvents, it generates little to no Volatile Organic Compounds (VOCs) during curing, offering a high utilisation and minimal waste disposal [38]. The ability to store powder epoxy in a glassy state under ambient conditions is made possible by the inclusion of latent curing agents in its composition, resulting in a prolonged shelf life and making it ideal for use in environments with low air and moisture content [32,39].

The traditional method of applying FR on composites involves uniformly coating each layer of fibres, which results in high costs associated with the FR mass, but also negatively affects their mechanical properties. Therefore, a minimal FR dose is typically favoured as more than 10 percent by weight (wt%) addition will negatively impact the mechanical properties [40]. Researchers have historically focused on developing new FRs [11–19] but have not adequately studied how the distribution of FR within the composites can be optimised. To the knowledge of the authors, there has been only one study conducted by Liao et al., in 2017 that investigated the fire retardancy of FR glass fabric-reinforced epoxy resin laminates prepared via different distribution modes [41]. The FR used were a combination of Melanine Polyphosphate (MPP) and Aluminium diethyl phosphinate (AlPi) with a fixed mass ratio of 1:2 where the comparison is made based on the charring capacity. The study compared the fire retardancy of laminates manufactured using a gradient distribution mode with those manufactured using a traditional uniform distribution mode. In comparison to the uniform distribution mode, where the FR is evenly distributed throughout each layer of the laminate, the gradient distribution mode focuses a higher concentration of FR on the surface while gradually decreasing the concentration across the layer of the laminate. The study found that, when the same volume fraction of FR was applied, the laminate manufactured with the gradient distribution mode exhibited better fire performance (i.e., higher LOI with lower FR content). This was achieved by the surface layer of the laminate exhibiting increased charring capacity, effectively protecting the underlying layers. Notably, the laminate with the gradient distribution mode achieved this with a lower FR content compared to the one manufactured using the uniform distribution mode. However, several aspects necessitate further investigation, including the type of FR used, the concentration of FR at the topmost layer of the laminate, and the potential variations in results associated with the use of powder-based epoxy laminates.

FRs that exhibit intumescence effect, i.e., those which expand to form a protective char layer when exposed to heat, are particularly effective in the initial stages of combustion, limiting heating and pyrolysis of the polymer resin [42,43]. The charring behaviour of epoxy based composite materials is therefore crucial in determining the effectiveness of incorporating FR in the composite [44]. The process of charring regulates the rate of heat transfer into the solid due to the lower effective thermal conductivity of the char layer compared to the epoxy. This phenomenon is particularly evident in materials like wood, where the char layer plays a crucial role in determining the burning behaviour and by extension the fire performance [45,46]. By promoting the formation of a thick char layer, a FR on the surface can reduce or prevent the pyrolysis of internal layers of the composite [42]. Therefore, this project will introduce the top-most distribution mode, where the FR will be concentrated only on the surface of the laminate to promote this charring effect at the surface. This will be compared to the gradient and uniform distribution mode. In addition, powder epoxy will be employed instead of the conventional liquid epoxy. Using powder epoxy enables the precise C; 0;0 of the ratio of powder epoxy to FR, making it possible to create a gradient in the composite layers that is difficult to achieve with liquid epoxy [32].

FR can be incorporated into a polymer matrix in two ways - additive and reactive. Most research in the last decade has focused on using additive FR compounds to improve the fire performance of glass/epoxy composites [26,27,41,47–49]. This method involves adding FR compounds to the polymer matrix, resulting in a uniform FR dispersion within the matrix [47]. However, the drawback of this approach is the weak compatibility between the FR and the polymer, which often leads to a reduction in the mechanical properties of the composite [48]. Although many of these additives have resulted in unfavourable modifications to the mechanical properties, ammonium polyphosphate (APP) and melamine polyphosphate (MPP) have been found to be an exception [26,27,47]. Matykiewicz et al. found that when both MPP and APP are present at the same wt%, MPP has a greater impact on enhancing the mechanical strength [27]. They also discovered that adding 20 wt% of MPP to the glass/epoxy composite decreased strength by 3%, while using a lower amount of 5 wt% MPP resulted in a 11% increase in strength. This suggests that only a minimal dosage of MPP is needed to achieve effective fire retardancy while retaining its mechanical properties. Additionally, the low cost of MPP makes it an attractive option to the fire retardancy of a specific material without incurring significant additional expenses [50,51].

The modification of polymer backbones with reactive FR compounds is another approach to enhance the fire performance of glass/epoxy composites. This method is more effective than using additive FR compounds, as the reactive FRs are integrated into the polymer structure [52,53]. The incorporation of these compounds does not affect the thermal stability or mechanical properties of the composite, but it does increase manufacturing costs [53]. Studies in recent years have investigated the impact of reactive FRs on the fire performance of glass/epoxy composites, with promising results reported in the literature [54–57]. However, one compound that has shown both excellent impact on both fire and mechanical properties of composite materials is 9,10-dihydro9-oxa-10-phosphaphenanthrene-10-oxide (DOPO) [54]. DOPO has gained much attention in recent years as a popular halogen-free FR [55]. It is easily accessible and commercially available on a large scale [56]. Its high thermal stability and ability to achieve effective fire retardancy in small dosage makes it a preferred choice as a reactive FR for glass/-epoxy composite [56,57].

Wang et al. conducted a study that compared the impact of adding an additive (MPP) and a reactive (DOPO) FR on the thermal, mechanical, and fire properties of glass fibre reinforced epoxy composites [25]. The results showed that DOPO was more efficient in decreasing flammability (i.e. the peak heat release rate (pHRR) and the total heat release (THR) as compared to MPP). This is because DOPO operates in both the condensed and gaseous phases, whereas MPP primarily interacts physically in the condensed phase [25,58,59]. Incorporating MPP led to a decrease in the modulus and tensile strength, whereas DOPO resulted in a slight increase in modulus and had a minimal effect on the strength. This may be attributed to the lower cross-linking density of epoxy/DOPO, which altered the flow behaviour of the polymer during the manufacturing of the composite, resulting in improved fibre wetting and increased fibre-matrix interaction [25]. In summary, the study found that DOPO, as compared to MPP, provided better fire retardancy properties while maintaining the mechanical strength of the composite. Another study has also been conducted by Neumeyer et al. on the influence of DOPO on the flammability behaviour of an epoxy novolac-based hot-melt prepreg resin system cured with dicyandiamide through UL94 testing [60]. It reveals that as the amount of DOPO increases, the glass transition temperature decreases due to a reduction in network density caused by the reaction of DOPO with epoxy groups [60]. However, the fracture toughness and elastic modulus of the resin remain largely unaffected within the examined range [60]. Notably, the incorporation of DOPO leads to improved flame resistance, as evidenced by UL 94 testing [60].

Despite the progress in novel flame retardants for epoxy composites, optimal fire performance depends not only on the chemical nature of the retardant but also on its distribution within the laminate structure. Recent studies demonstrate that concentrating phosphorus-based fire retardants, such as DOPO, at the surface or in tailored gradients can promote charring and delay peak heat release while efficiently reducing

overall additive usage. This work expands on surface and gradient distribution approaches, specifically using powder epoxy to achieve precise fire-retardant concentration profiles, and systematically compares their effects on cone calorimetry metrics. The findings show that, compared to traditional uniform incorporation, gradient and top-mode distribution of DOPO significantly enhance fire retardancy at lower total loadings, underscoring the importance of through-thickness optimization and providing a framework for balancing cost, fire performance, and mechanical properties. These results complement earlier work by Liao et al. [41] and Wang et al. [60], but demonstrate for the first time the practical and scalable application using powder epoxy–enabling tailored, sustainable composite manufacturing routes for advanced fire-safe engineering structures.

2. Experimental

2.1. Materials

The specific DOPO used in the experiment was OR53111, supplied by Apollo Scientific based in Stockport, United Kingdom. The DOPO has a melting point of 119°C, a density of 1.4 g/cm3, and comes in the form of white flakes [61]. The glass fibre used as the reinforcement in manufacturing the plates was a 591 gsm UD stitched glass fabric from SAERTEX based in Saerbeck, Germany. The density of the glass fibre is 2.6 g/cm^3. A Benzoxazine powder epoxy (PE6405) which was produced by FreiLacke in Bräunlingen, Germany was chosen as the matrix for the GFRP plates. The powder epoxy has a density of 1.2 g/cm^3. An interesting aspect of powder epoxy is its ability to melt at around 50°C but only start curing at 150°C through a heat activated process. This enables a superior control over the dispersion of additives within composite systems.

2.2. Plate preparation

Three distribution modes of DOPO are investigated, and for each mode, the overall DOPO volume fraction will vary within the range of 2.5% to 20%. The total volume of DOPO in each layer of the GFRP plates will vary depending on its distribution modes, resulting in variations in the overall DOPO volume fraction. These variations in Fibre Volume Fraction (FVF) content in each distribution mode will have a significant impact on the flammability of the GFRP plates. It is therefore crucial to analyse and understand the effects of these variations to determine the effect of DOPO fraction and distribution modes. Additionally, determining the point at which adding more DOPO no longer has an effect is essential for reducing waste and unnecessary costs while maintaining the desired fire performance. The type of plates that are manufactured for each distribution modes with varying overall DOPO volume fraction is summarised in Table 1.

The GFRP plates were manufactured using a manual layup method. A steel frame with 8 mm thickness and inner dimensions of 300 mm × 280 mm served as the mold, secured with tacky tape and two steel caul plates as shown in Fig. 1. The mold was coated with polytetrafluoroethylene (PTFE) to aid plate removal after curing. The glass fibre plies each

Table 1
Types of plates available for each distribution mode with varying FVF of DOPO.

Overall DOPO Volume Fraction (%)	Type of Distribution Modes			
	Control	Homogenous	Gradient	Top
0	X			
2.5				X
5		X	X	X
10			X	X
20		X	X	

Abbreviations: Fibre Volume Fraction (FVF), 9,10-dihydro-9-oxa-10-phosphaphenanthrene-10-oxide (DOPO).

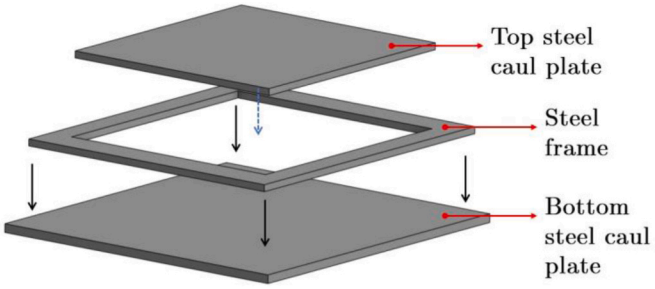

Fig. 1. Schematic of the mold used for layup.

measuring 300 mm × 280 mm, were cut using a shear scissor. Eight layers of plies were used for each plate. The mass of powder epoxy and DOPO for each interply layer was weighed based on specified concentrations for each distribution mode.

In preparing the control plate, powder epoxy was evenly scattered onto each fabric layer to ensure good fibre wetting and uniform resin distribution (Fig. 2). For the homogeneous plate, specified amounts of powder epoxy and DOPO for each interply layer were weighed, mixed in a sealed bag, and applied uniformly on top of each fabric layer (Fig. 3). In the gradient mode, the ratio of powder epoxy to DOPO varied for each layer, with DOPO content gradually decreasing from the first to subsequent layers (Fig. 4). In the top-most distribution mode, only the first layer was mixed with DOPO, while the remaining layers were sprinkled with powder epoxy, concentrating DOPO on the surface layer (Fig. 5).

The curing process follows the layup, using a SciQuip Oven-230HT and the vacuum bagging method. The vacuum bag is placed inside the oven under a 1-bar vacuum pressure to ensure consolidation and eliminate voids (Fig. 6). The curing cycle as presented by Fig. 7 includes drying the powder at 40°C for 8 h, then raising the temperature to 120°C for an hour to liquefy the powder and achieve optimal wetting. The plate is then post-cured at 180°C for 2 h and gradually cooled to room temperature over 3 h. After cooling, the plate is removed from the oven to avoid thermal stresses.

Table 2 summarises the types of plates available for each distribution mode with varying volume fraction of DOPO. Henceforth in this study, the plates will be denoted by acronyms for reader convenience. The acronym format is A; B;C, where A denotes the distribution mode, B signifies the overall DOPO volume fraction, and C represents the DOPO volume fraction of the topmost surface layer of the plate. For example, a plate labelled as H; 5;2.5 indicates a homogeneous plate with an overall DOPO volume fraction of 5%, and a surface layer with a DOPO volume fraction of 2.5%.

2.3. Flammability test

The flammability testing is conducted using the cone calorimeter according to the principles set out in ISO 5660 [62] to examine the time

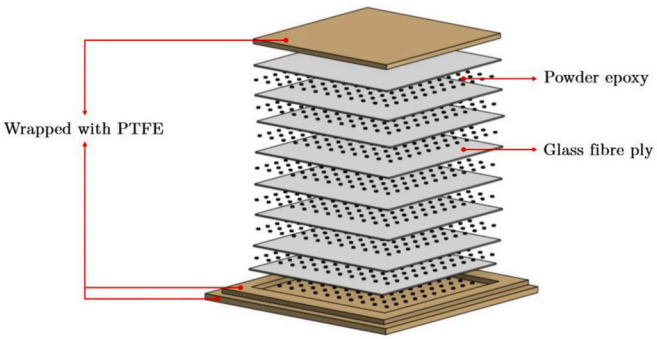

Fig. 2. The control plate.

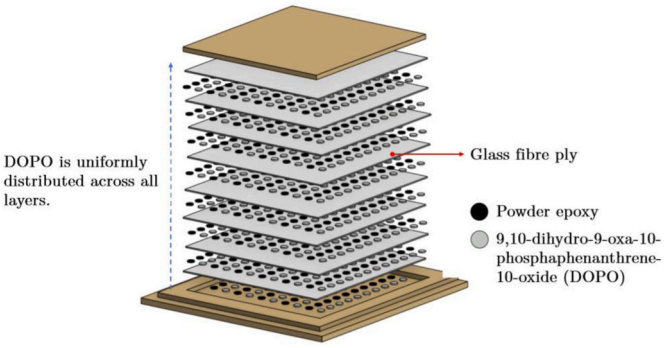

Fig. 3. The homogenous plate.

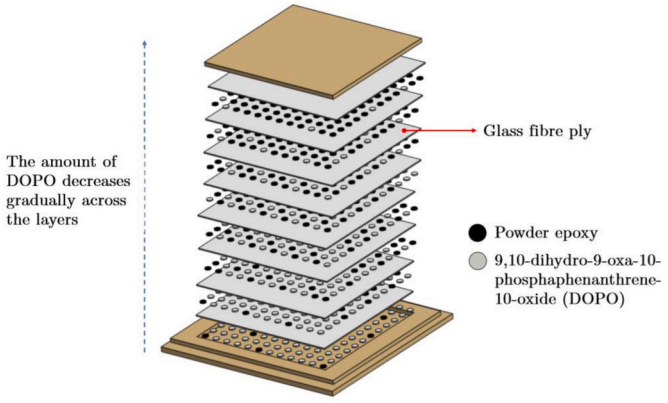

Fig. 4. The gradient plate.

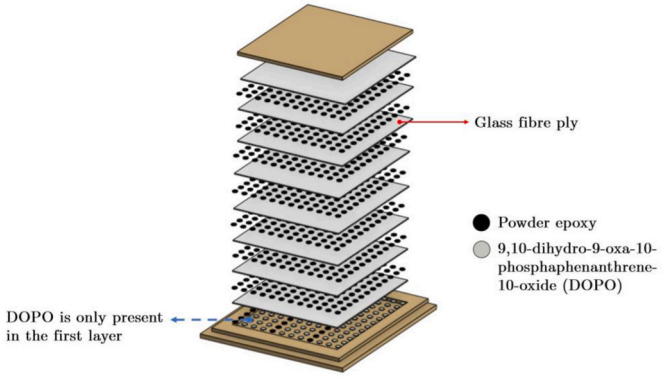

Fig. 5. The top plate.

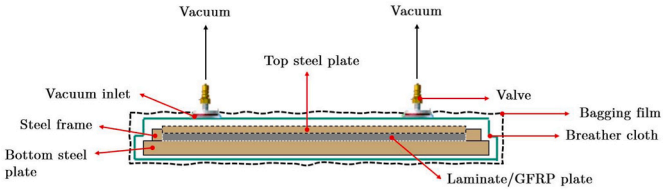

Fig. 6. Schematic of the cross-sectional view of the vacuum bagging.

to ignition, heat release rates, and gaseous emissions of the manufactured GFRP plates [63]. A heat flux of 35 kWm^{-2} is used. The cone calorimetry tests were carried out an average of three times for each plate, providing a general indication of the repeatability of the results

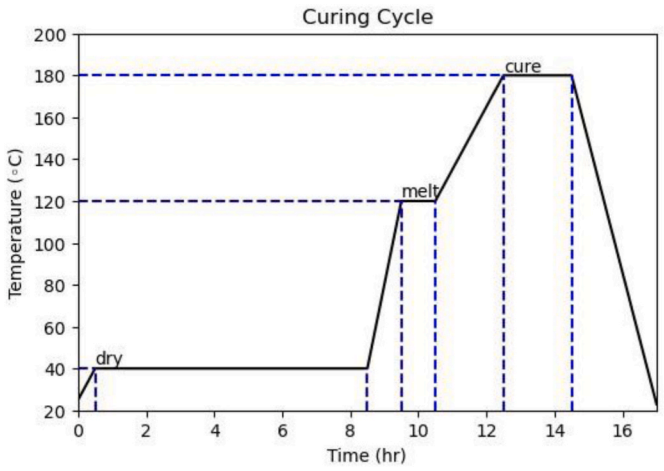

Fig. 7. The graph shows the curing cycle of the plate.

Table 2
Types of plates available for each distribution mode.

Type of Plates	Overall DOPO Volume Fraction (%)	Top Surface Layer DOPO Volume Fraction (%)	Acronyms
Control	0	0	C; 0;0
Homogeneous 5%	5	2.5	H; 5;2.5
Homogeneous 20%	20	10	H; 20; 10
Gradient 5%	5	10	G; 5;10
Gradient 10%	10	20	G; 10; 20
Gradient 20%	20	40	G; 20; 40
Top 2.5%	2.5	10	T; 2.5; 10
Top 5%	5	20	T; 5;20
Top 10%	10	40	T; 10; 40

across trials, except for H; 5;2.5 and T; 2.5; 10 plates.

To prepare for testing, a 100 mm × 100 mm plate is positioned within a sample holder comprising a pan and retainer frame. The bottom boundary of the GFRP plate is insulated with ceramic paper. Prior to placement, aluminium foil is used to wrap each plate. Components within the sample holder are detailed in Fig. 8. The measurements subjected to analysis in these tests include the heat release rate (HRR), carbon monoxide (CO) generation and time to ignition (TTI), with the HRR being calculated by oxygen consumption calorimetry [64].

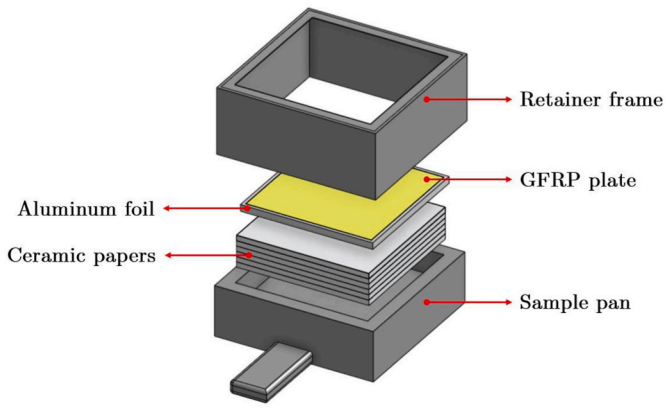

Fig. 8. Schematic of the sample holder.

3. Results and discussion

3.1. Visual observations

Each specimen was ignited and allowed to burn to completion (i.e., negligible measured change in mass). As shown in Fig. 9a, after burning, the C; 0;0 plate leaves only a minimal residual char around the sample edges where the sample holder would result in cooling of the epoxy. In contrast, the H; 5;2.5 plate (Fig. 9b) exhibits a more residual char, while increasing the DOPO content to 20% (Fig. 9c) results in greater char residue. This pattern extends to gradient and top distribution modes, where increased DOPO leads to more residual char. As previously described, DOPO's properties enable the formation of a protective char layer that acts as a heat transfer barrier. The G; 5;10 plate indicates a larger proportion of the surface covered in a char layer (as indicated in the blackened regions) due to the higher DOPO concentrations. The char formed on the T; 2.5; 10 plate (Fig. 9g) resembles G; 5;10 and H; 20; 10 plates (Fig. 9d and c), given identical surface DOPO concentration. In contrast, the T; 10; 40 plate exhibits a complete char layer with no fibres visible due to its highest surface DOPO concentration, suggesting that top-layer DOPO presence can yield a superior char layer reducing heat transfer into the specimen.

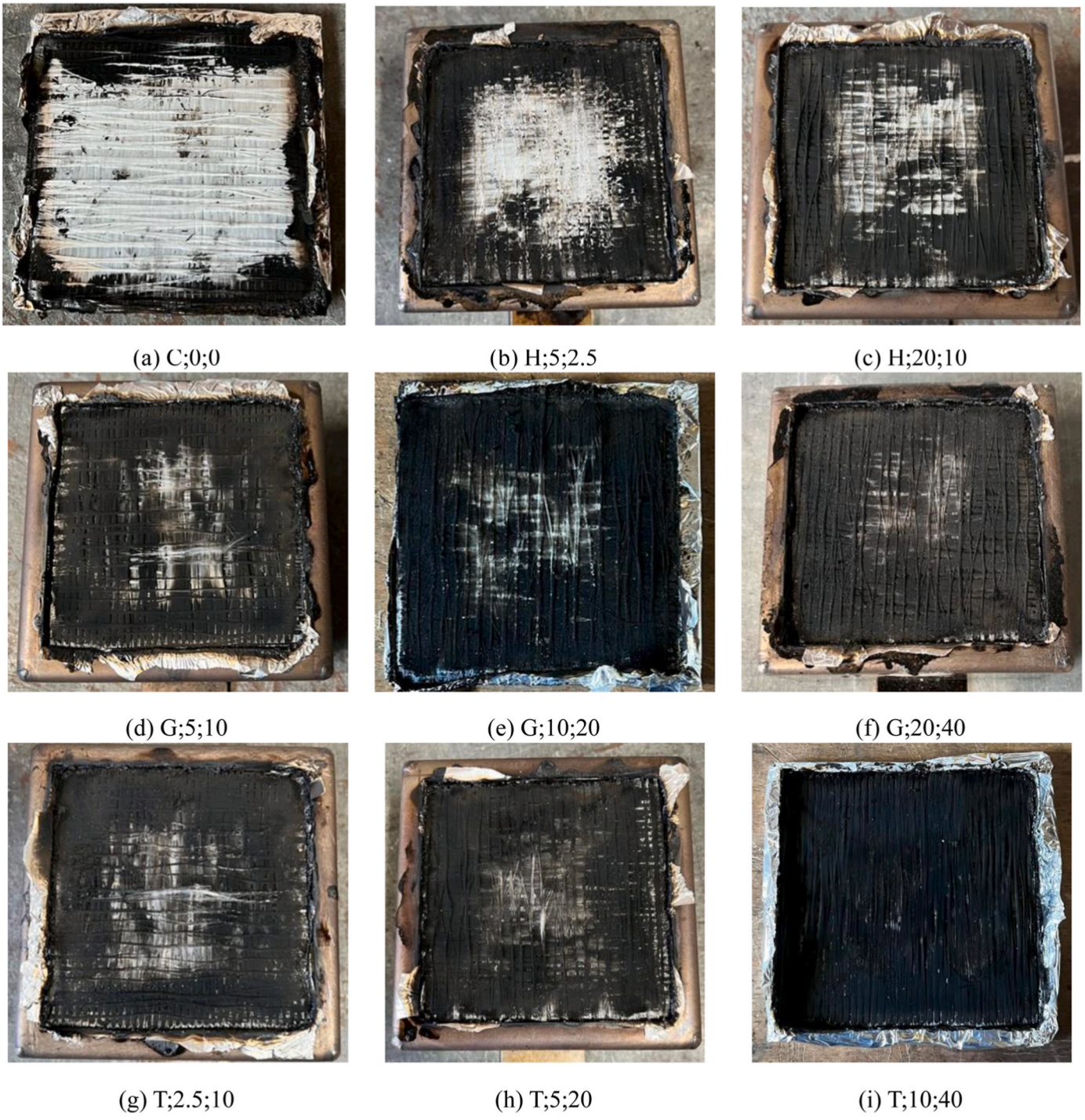

Fig. 9. Digital photographs of the residues of the plates after the cone calorimetry testing.

3.2. Time to ignition (TTI)

TTI results are presented in Table 3. This shows that the incorporation of DOPO decreases the TTI of the plates, regardless of the distribution mode, indicating that increasing the total volume of DOPO i.e. higher surface concentration leads to a systematic reduction in the TTI. As shown in Table 3, the C; 0;0 plate without DOPO has a higher TTI than all the samples with DOPO. The TTI decreases from 114 s to 95 s as the total volume of DOPO increases from 5% to 20% in the homogeneous plates. A similar trend is observed for the gradient and top plates, where an increase in the total volume of DOPO leads to a decrease in TTI.

This decrease in time to ignition is attributed to the fact that DOPO is designed to promote the formation of a char layer and hence readily decomposes at lower temperatures resulting in the release of flammable volatile species [25]. This is consistent with the work of by Qian et al. [65] and Huo et al. [66] where the incorporation of DOPO decreased the TTI. By promoting char formation, the time to ignition is reduced. This highlights the need to clearly understand the aims of material modification to achieve the desired fire safety outcomes i.e. reduced TTI or reduced HRR.

3.3. Heat release rate (HRR)

Cone calorimetry was carried out an average of three times for each plate, providing a general indication of the repeatability of the results across trials, except for H; 5;2.5 and T; 2.5; 10 plates. To facilitate discussion, one typical HRR curve was chosen to highlight transient aspects (such as local peak HRR) which can occur at different times between each experiment; as such taking an average across all trials loses insight into comparing these key results.

3.3.1. Influence of DOPO volume fraction variation

Fig. 10 presents the HRR curves for three distinct distribution modes with varying total volume of DOPO: (1) homogeneous, (2) gradient, and (3) top. The HRR curve of the C; 0;0 plate is provided for comparison in each sub figure. Notably, the absence of DOPO in the C; 0;0 plate results in a high peak HRR after ignition, and a single distinct pHRR of 2.84 kW is observed at 180s. It is evident that the addition of DOPO results in a reduction of both the pHRR and THR values. The pHRR and THR obtained from the cone calorimetry testing for all the plates are summarised in Table 4.

Fig. 10a compares HRR curves between two plates under homogeneous distribution mode. It can be seen that addition of 5% or 20% DOPO leads to shorter times to ignition (indicated by earlier increases in the HRR) with higher DOPO concentrations resulting in shorter times to ignition. However, larger DOPO concentrations result in lower pHRR and shorter burning durations (before the decrease in HRR). The lower pHRR is attributed to the formation the char layer promoted by DOPO, which reduces heat transfer into the solid and increases surface heat losses. Fig. 11 and Table 4 shows the pHRR and THR from each sample.

Table 3
Summary of TTI values obtained from cone calorimetry testing.

Type of plates	TTI (s)
C; 0;0	125
H; 5;2.5	114
H; 20; 10	95
G; 5;10	107
G; 10; 20	104
G; 20; 40	97
T; 2.5; 10	119
T; 5;20	112
T; 10; 40	110

Abbreviations: Time to Ignition (TTI).

Increasing the DOPO concentration decreases the THR by approximately 36.2% and 49.5% for the H; 5;2.5 and H; 20; 10 plates respectively.

Similarly, in the gradient distribution mode (Fig. 10b), increasing DOPO content from 5% to 20% decrease pHRR and THR. The G; 10; 20 plate shows similar HRR behaviour to the G; 5;10 plate for the first 250s, however the G; 5;10 plate shows a secondary peak in HRR and a longer burning duration. The G; 20; 40 plate exhibits a slower rise in HRR to the peak due to significant char formation (Fig. 10b).

Fig. 10c shows the HRR for the top plate samples. In this case the differences in HRR are not as pronounced as for the homogeneous and gradient cases. In general, increasing DOPO concentrations resulted in a decreased pHRR over the duration of the experiment. However, it is worth noting the same trend was not observed for the HRR behaviour between 0 and 250 s. The T; 5;20 plate displayed a slower increase over the 0-250s period compared to the T; 10; 40 plate. However, beyond 250s, the anticipated behaviour between each case was observed (i.e., higher pHRR and longer burning duration for the T; 5;20 plate). The difference in the growth to the peak HRR for the T; 5;20 plate may be due to differences in laminate manufacturing but would require further investigation to determine.

These results indicate that adding beyond a threshold value, more DOPO provides only incremental enhancement in fire-retardant properties. Consequently, it becomes crucial to identify the optimal DOPO quantity required to achieve the targeted fire performance.

DOPO reduces the Effective Heat of Combustion (EHC) primarily by altering the combustion pathway: it promotes intensive char formation via phosphoric acid generation and traps flame-propagating radicals in the gas phase. The phosphorus-based DOPO acts both in the condensed phase, accelerating dehydration and carbonization, and in the gas phase, quenching energetic radicals to suppress the burning of volatile organic gases. This dual mechanism lowers the energy released per unit mass and results in less complete combustion, hence a lower EHC as FR content increases.

3.3.2. Influence of distribution mode for equal total volume of DOPO

Fig. 12a displays HRR curves for H; 5;2.5, G; 5;10, and T; 5;20 plates, indicating the T; 5;20 plate has the lowest initial HRR, followed by G; 5;10 and H; 5;2.5. Over time, both G; 5;10 and T; 5;20 plates reach the same pHRR, but the TTI is faster for the T; 5;20 plate, due to the higher DOPO fraction at the surface. The results in Fig. 12a particularly highlight the reduction in HRR during the growth to the peak, i.e. 0-250s, when the FR is preferentially loaded towards the surface of the sample, as seen in either the top or gradient configurations. Similarly, for G; 10; 20 and T; 10; 40 plates in Fig. 12b, pHRR and THR values are comparable but the gradient case results in a shorter period of burning at high heat release rate. Regarding 20% total volume DOPO plates (Fig. 12c), the H; 20; 10 plate shows a more rapid increase to the pHRR compared to the G; 20; 40 plate due to the higher concentration of DOPO near the surface in the latter case. This underscores gradient distribution's efficacy in delaying combustion and highlights that surface concentrated DOPO forms a thicker, more effective char layer, consistent with findings from Fig. 12a and b.

3.3.3. Influence of distribution mode for equal surface layer concentration

Fig. 13 displays the HRR curves of the plates with the same surface layer concentration. For instance, Fig. 13a depicts the HRR curves for plates with a surface layer concentration of 10%. The T; 2.5; 10 plate has the highest pHRR and THR compared to the other plates with DOPO. This indicates that 2.5% total DOPO volume, with 10% of DOPO on the surface, is sufficient to have an effect in reducing flammability as evidenced by a 25.7% decrease in pHRR and 25.3% decrease in THR when compared to the C; 0;0 plate. The H; 20; 10 plate demonstrates the lowest pHRR and THR, requiring a 20% total DOPO volume to achieve this effect. Compared to the control plate, the pHRR decreases by 47.2%, and the THR drops by 49.5%. However, it is crucial to highlight that achieving these results necessitates a 20% total DOPO volume. In

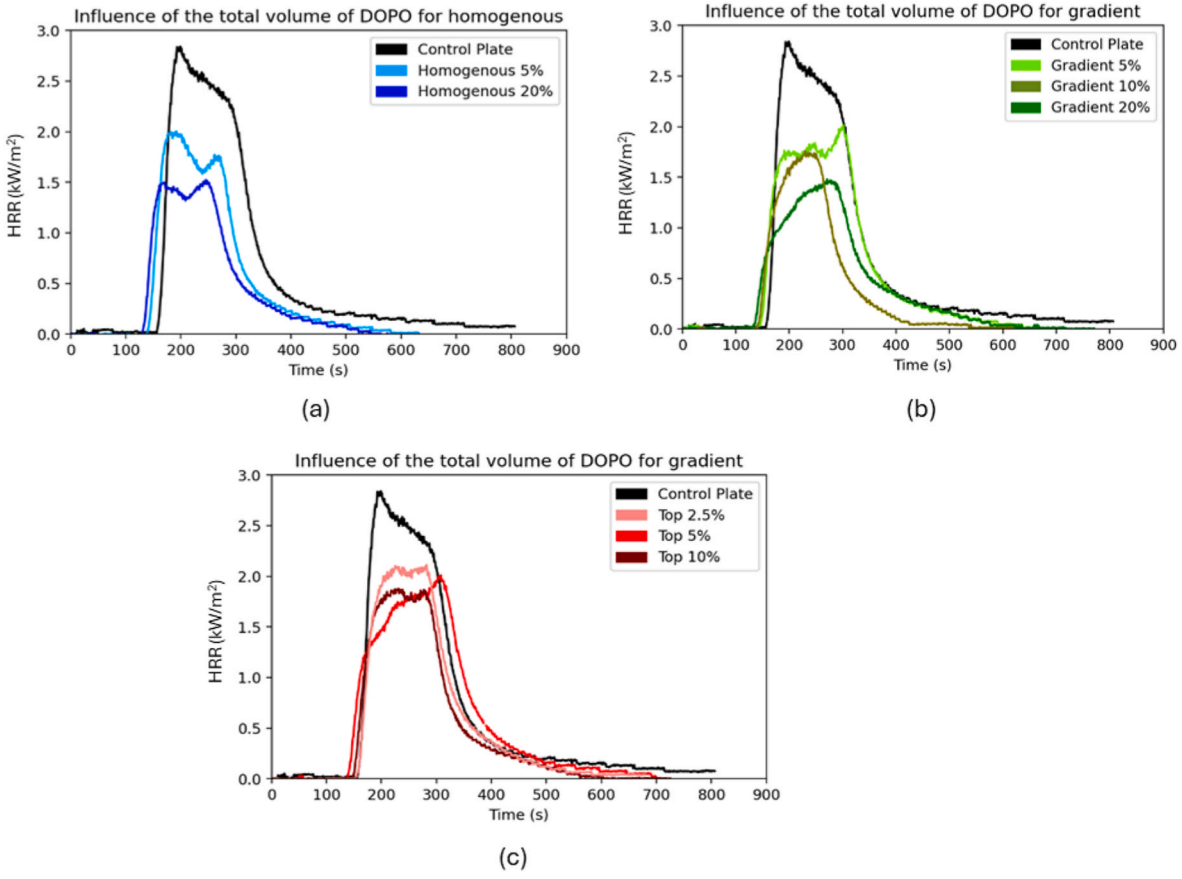

Fig. 10. Typical HRR curves for a) homogeneous, b) gradient, and c) top plates.

Table 4
Qualitative values of pHRR and THR for each plate.

Type of Plates	Overall DOPO Volume Fraction (%)	pHRR (kW)	THR (MJ)
C; 0;0	-	2.84	477.8
H; 5;2.5	5	2.00	304.9
H; 20; 10	20	1.50	241.4
G; 5;10	5	1.98	366.9
G; 10; 20	10	1.73	282.4
G; 20; 40	20	1.46	238.3
T; 2.5; 10	2.5	2.11	356.7
T; 5;20	5	1.88	354.0
T; 10; 40	10	1.77	319.1

Abbreviations: peak Heat Release Rate (pHRR), Total Heat Release (THR).

Fig. 13b, the HRR curves for G; 10; 20 and T; 5;20 plates, both featuring a 20% surface layer DOPO concentration, exhibit lower pHRR and THR values compared to the C; 0;0 plate. Despite the initial stages of both samples being similar, the G; 10; 20 plate achieves lower pHRR and THR than the T; 5;20 plate. This difference could be attributed to the G; 10; 20 plate having a higher total volume compared to the T; 5;20 plate. Similarly, this scenario reflects the findings in Fig. 12a, wherein the T; 5;20 plate, despite having a lower total volume than the G; 10; 20 plate, could attain satisfactory results by concentrating all DOPO on the surface.

The same pattern is observed in Fig. 13c, which presents HRR curves for G; 20; 40 and T; 10; 40 plates with a 40% surface layer DOPO concentration. The G; 20; 40 plate, distributing 40% DOPO on the top layer, exhibits the most significant reduction in pHRR due to its higher total DOPO volume across the layers. In contrast, the T; 10; 40 plate's limited surface DOPO leads to a higher peak but similar burning duration. Upon examination of Fig. 13, it becomes apparent that while gradient plates typically display the lowest pHRR and THR due to their higher total

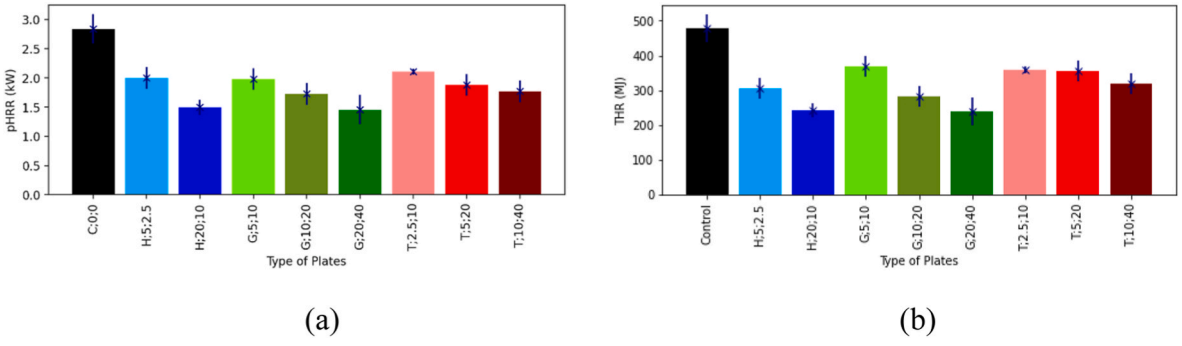

Fig. 11. (a) The pHRR and (b) THR values for each plate.

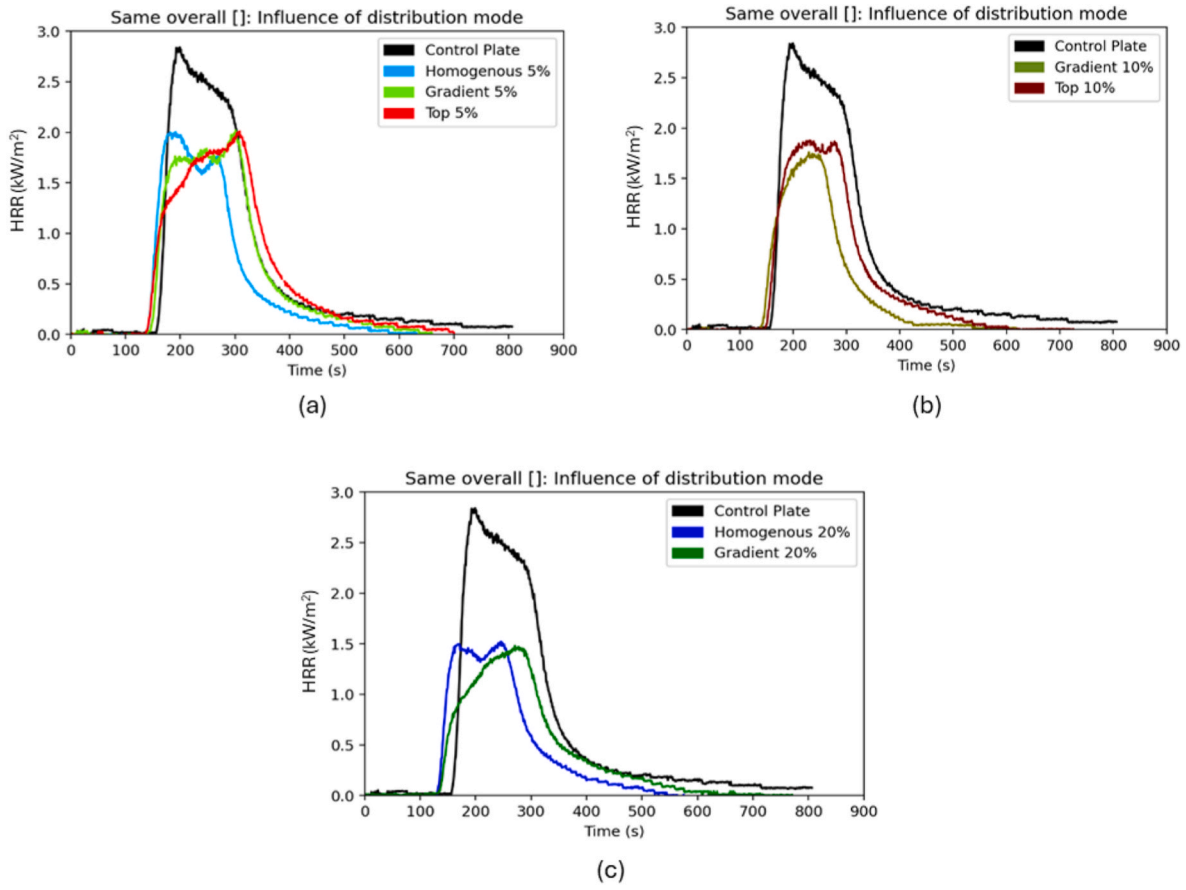

Fig. 12. Typical HRR curves for total volume DOPO of a) 5%, b) 10%, and c) 20%.

DOPO volume, a different perspective emerges when focusing solely on distributing DOPO on the surface layer, as demonstrated by the top plates. This suggests that focusing DOPO application close to the surface offers opportunities for optimizing FR loadings and cost with fire performance. Additionally, the growth rate of peak HRR is slower for the top plates, indicating that distributing DOPO on the surface layer has an impact on the fire performance.

3.4. CO generation

The HRR data presented in Figs. 10–12 demonstrate the reduction in HRR with the addition of DOPO. This may be due to a reduction in the mass loss rate as the char layer is formed and/or changes in the gas phase chemistry. Fig. 14 illustrates the CO generated from the plates, and the average CO yield is presented in Table 5. The addition of DOPO is shown to result in increased CO yields across all conditions tested. Fig. 14a reveals that increasing the total DOPO volume from 5% to 20% in homogeneous plates elevates CO production due to the role of DOPO in generating a char layer and decreasing the completeness of the gas phase combustion. The observed increase in CO yield upon addition of flame retardant is technically attributed to enhanced char formation at the composite surface, which acts as a physical barrier limiting oxygen diffusion into the pyrolysis zone. When the char layer restricts oxygen ingress, the oxidation of volatile pyrolysis products is suppressed, resulting in incomplete combustion and a higher ratio of CO to CO_2. This mechanism is well established for phosphorus-based flame retardants like DOPO, where the protective carbonaceous layer impedes oxygen transport, favoring the formation of CO over full oxidation to CO_2. A similar pattern is observed in gradient plates (Fig. 14b), with the highest CO in the G; 20; 40 plate, where the surface DOPO concentration is highest. Increasing DOPO in the surface layer of G; 10; 20 and G; 20; 40 plates result in greater generation of CO. Correspondingly, Fig. 14c shows comparable results in top plates, except the T; 10; 40 plate displaying lower CO despite higher DOPO content, indicating excessive DOPO beyond 5% might not yield additional benefits. While the results in Fig. 14 highlight the change in CO generation for each of the configurations tested, CO mass flow alone does not account for the change in the CO yield (i.e., the amount of CO generated as a function of the burning rate).

Average CO yields were calculated as a ratio of the total CO generation (g) to the total mass lost (g) from the start of test t = 0s to t = 400s. The results for each configuration are presented in Fig. 15. The yield of CO was found to increase with increasing DOPO concentration, with the H; 20; 40 plate trails showing an order of magnitude higher yield compared to the C; 0;0 plate. This relationship suggests there is potential to optimize the HRR reduction and increase in CO yield for any FR treatment technique. One example of this can be seen in comparing the H; 20; 40 plate to the G; 20; 10 plate which both show relatively similar HRR data (Table 4) while the CO generation for the homogenous case (as seen in Figs. 14b and 15) produces significantly more CO. It is also notable that, in the case of plates with top distribution, there is a noteworthy rise in CO yield from 2.5% to 5% total volume DOPO, followed by a subsequent decline at 10% total volume DOPO. This phenomenon can be linked to the early peak in CO yield for the top plates, despite the HRR exhibiting a considerably delayed peak. The implications of this on the average CO yield remain uncertain. Despite that, it can be asserted that the CO yield for each plate with DOPO surpasses the control plate (C; 0;0), indicating that the presence of DOPO increases the CO yield. These results highlight that the optimization of FR treatments must consider a balance of factors including HRR, smoke toxicity (e.g., CO), and cost of manufacturing.

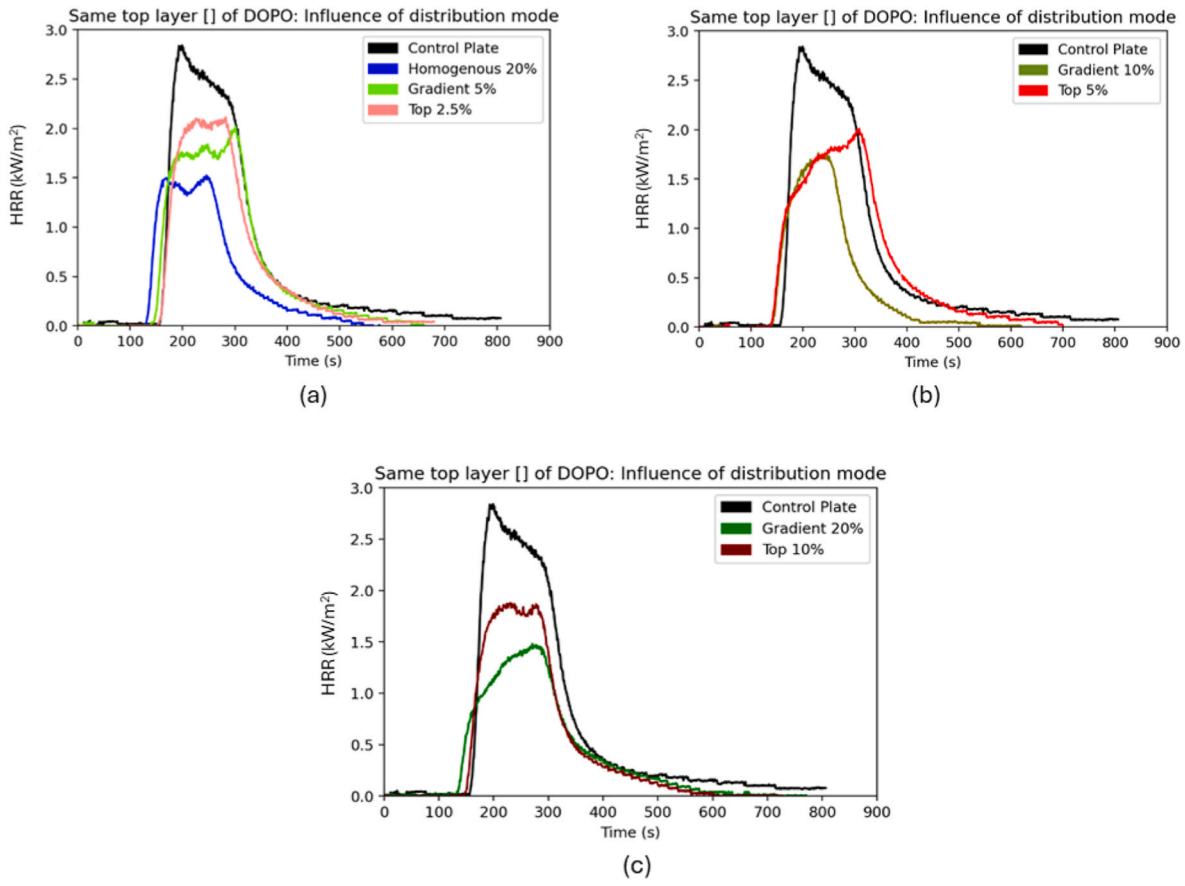

Fig. 13. Typical HRR curves for surface layer concentration for DOPO of a) 10%, b) 20%, and c) 40%.

3.5. *Effective Heat of Combustion*

The analysis of the average Effective Heat of Combustion (EHC) trends observed in Table 5 indicates that the incorporation of DOPO as a FR in varying fractions and distribution modes effectively reduces the energy released per unit mass of the material pyrolyzed. The EHC for standard epoxy resins typically ranges from 20 to 30 MJ/kg [67]. However, incorporating FR can significantly lower the EHC. For instance, adding phosphorus-based FR like cyclotriphosphazene microspheres to epoxy resins can reduce the EHC by promoting char formation and reducing the release of combustible gases [67]. In one example, the EHC was reduced from 24.2 MJ/kg to 22.9 MJ/kg with a 5% addition of such FR [67]. In the case of DOPO, the reduction in flammability is attributed to the promotion of charring by phosphorus in the condensed phase [68]. Phosphorus acts as a catalyst for char formation [68].

EHC is thus calculated by dividing the THR by the total mass loss (TML). Lower EHC values suggest that not only is less mass being lost, but also less energy is being released per unit of fuel (i.e., less energetic release from the volatile gases). A reduction in EHC can be used as an additional metric for the performance of the FR. For any given condition (e.g., the homogenous distribution), Table 5 indicates that the EHC decreases with increasing FR quantity. This result suggests DOPO's efficacy in reducing the heat release rate per unit mass pyrolyzed. It is worth noting that the homogeneous distribution shows the lowest EHC values, the with gradient trials showing only marginally higher values. The top distribution mode was shown to have the highest EHOC for each total DOPO loading.

4. Conclusions

This study demonstrates that the fire performance criteria of a material are influenced by various FR distributions, namely homogeneous, gradient, and top distribution. The findings suggest the potential for optimizing the material based on these distributions, opening avenues for further improvement in fire performance. Among plates with the same distribution mode, a higher DOPO content led to decreased HRR. In comparison to the control plate without DOPO, the gradient plate with 20% total volume DOPO exhibited a 50.1% reduction in THR and a longer delay reaching pHRR. The primary mechanism by which DOPO promoted lower HRR was through promoting char formation; as such, loading DOPO at the surfaces through the gradient and top configurations were beneficial in promoting charring at the surface. However once char had formed, the DOPO throughout the remaining laminate had only marginal benefit in reducing the HRR under the conditions tested. The reduction in HRR with the addition of higher DOPO concentrations has found to be nonlinear with total DOPO concentrations (i.e., additional DOPO concentrations only marginally reduced the HRR). It is also worth noting that the highest concentration for the top plate (T; 10; 40) does not follow the upward trend, but it is still higher than the baseline case so there is still a need to optimize the DOPO concentration. Thus, determining the optimal concentration of DOPO is crucial, as adding more does not guarantee better results. Furthermore, it can be inferred that adding DOPO increases the production of CO and reduces the TTI values.

It is self-evident that the addition of more FR will reduce factors such as the pHRR and THR. However, such reductions in one factor should be balanced with the subsequent increase in other factors (e.g. ease of ignition, generation of products of incomplete combustion and cost). The highest concentrations of DOPO were found to increase the CO yield of the laminates by an order of magnitude; as such, this work outlines key flammability metrics such as HRR, TTI and CO generation which can be balanced in the design of FR composites. The application of DOPO in

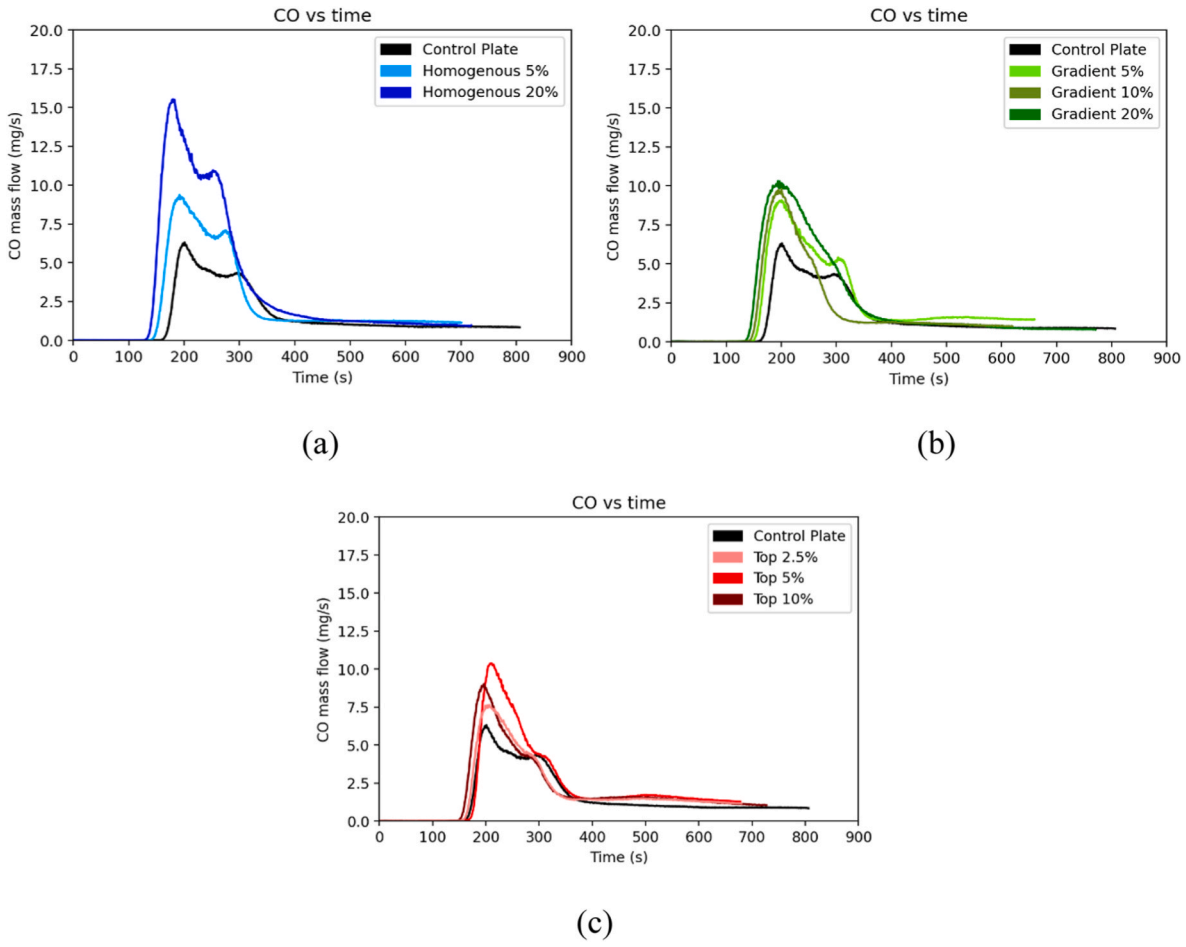

Fig. 14. Typical CO curves for a) homogeneous, b) gradient, and c) top.

Table 5
Summary of EHC values for different types of plates.

Type of plates	Average EHC (MJ/g)
C; 0;0	21.4
H; 5;2.5	16.1
H; 20; 10	13.9
G; 5;10	17.9
G; 10; 20	16.9
G; 20; 40	16.4
T; 2.5; 10	20.5
T; 5;20	20.0
T; 10; 40	15.1

Abbreviations: Effective Heat of Combustion (EHC).

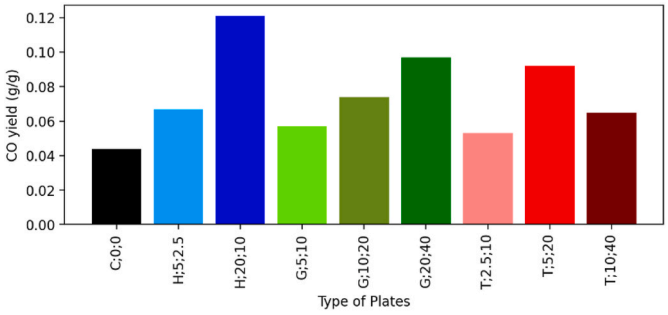

Fig. 15. Average CO yield for each plate.

a gradient mode and on the topmost layer has been demonstrated to reduce the HRR behaviour while maintaining the same total concentration of FR. Therefore, gradients of DOPO, or other fire retardant, concentration may offer opportunities to reduce the total FR requirement. As such, this work presents a framework for applying targeted concentrations of FR treatment at specific depths and evaluating the efficacy of such approaches and highlights the importance of balancing other flammability characteristics in the optimization of such FR treatments.

While this study demonstrates that optimizing fire-retardant distribution modes can markedly reduce flammability and material costs, but several limitations remain. Future research should consider the impact on mechanical properties, the long-term durability of the distribution layouts, and the interplay between FR placement and smoke toxicity, as high surface concentrations of DOPO can increase CO yields and lower ignition thresholds. Additional investigations should also explore automated gradient manufacturing techniques, other halogen-free retardants, and multi-factor trade-offs, to enable practical uptake of tailored FR distributions in large-scale composite applications.

CRediT authorship contribution statement

Zalia Zainol: Writing – original draft, Validation, Methodology, Investigation, Formal analysis, Data curation, Conceptualization. **David Morrisset:** Writing – original draft, Validation, Supervision, Resources, Methodology, Investigation, Data curation, Conceptualization. **Arun Kumar Alapati:** Writing – original draft, Validation, Supervision, Methodology, Investigation, Formal analysis, Data curation. **Conchúr M. Ó Brádaigh:** Writing – review & editing, Supervision, Resources.

Rory M. Hadden: Writing – review & editing, Supervision, Investigation, Data curation, Conceptualization. **Colin Robert:** Writing – review & editing, Supervision, Project administration, Methodology, Investigation, Formal analysis, Data curation, Conceptualization.

Ethical approval

NA.

Declaration of competing interest

They are no competing interests, and I have nothing to declare.

Acknowledgments

The authors thank FreiLacke I Emil Frei GmbH & Co. KG for kindly gifting the material used in this study.

Data availability

Data will be made available on request.

References

[1] Andrea Toldy, P. Niedermann, Gabor Szebenyi, Beata Szolnoki, Mechanical properties of reactively flame retarded cyanate ester/epoxy resin blends and their carbon fibre reinforced composites, Express Polym. Lett. 10 (12) (2016) 1016–1025.
[2] B. Shivamurthy, K Udaya Bhat, S. Anandhan, Mechanical and sliding wear properties of multi-layered laminates from glass fabric/graphite/epoxy composites, Mater. Des. 44 (2013) 136–143.
[3] Chun Shan Wang, Ching Hsuan Lin, Synthesis and properties of phosphorus-containing epoxy resins by novel method, J. Polym. Sci. Polym. Chem. 37 (21) (1999) 3903–3909.
[4] JA Reina Mercado, M. Galia, Flame retardant epoxy resins based on diglycidyloxymethylphenylsilane, J. Polym. Sci. Polym. Chem. 44 (19) (2006) 5580–5587.
[5] Yukyung Kim, Sanghyuck Lee, Hyeonseok Yoon, Fire-safe polymer composites: flame-retardant effect of nanofillers, Polymers 13 (4) (2021) 540.
[6] Haoxin Niu, Hafezeh Nabipour, Xin Wang, Lei Song, Yuan Hu, Phosphorus-free vanillinderived intrinsically flame-retardant epoxy thermoset with extremely low heat release rate and smoke emission, ACS Sustain. Chem. Eng. 9 (15) (2021) 5268–5277.
[7] Leng Yang, Miaojun Xu, Yue Sun, Bin Li, Simultaneously improving the thermal conductive and flame retardant performance for epoxy resins thermosets by constructing core-shell-brush structure and distributing of mwcnts in brush intervals, Polym. Adv. Technol. 31 (3) (2020) 589–601.
[8] Yanlong Sui, Lijie Qu, Peihong Li, Xueyan Dai, Qiangsheng Fang, Chunling Zhang, Ying Wang, Covalently functionalized graphene oxide wrapped by silicon-nitrogen-containing molecules: preparation and simultaneous enhancement of the thermal stability, flame retardancy and mechanical properties of epoxy resin nanocomposites, RSC Adv. 10 (24) (2020) 13949–13959.
[9] Lamei Chen, Tianyou Song, Jingyu Wang, Hui Shi, Jianwei Hao, Intrinsic flame-retardant epoxy resin composites with benzoxazine: effect of a catalyst and a low curing temperature, J. Appl. Polym. Sci. 136 (33) (2019) 47847.
[10] Fei Xiao, Kun Wu, Fubin Luo, Sa Yao, Maoping Lv, Haimei Zou, Mangeng Lu, Influence of ionic liquid-based metal-organic hybrid on thermal degradation, flame retardancy, and smoke suppression properties of epoxy resin composites, J. Mater. Sci. 53 (2018) 10135–10146.
[11] Mehran Alaee, Pedro Arias, Andreas Sjödin, Åke Bergman, An overview of commercially used brominated flame retardants, their applications, their use patterns in different countries/regions and possible modes of release, Environ. Int. 29 (6) (2003) 683–689.
[12] Gregory Morose, An overview of alternatives to tetrabromobisphenol a (tbbpa) and hexabromocyclododecane (hbcd), Lowell Center for Sustainable Production, University of Massachusetts, Lowell (2006). http://sustainableproduction.org/downloads/AternativestoTBBPAandHBCD.pdf.
[13] Wenchao Zhang, Xiangdong He, Tinglu Song, Qingjie Jiao, Rongjie Yang, The influence of the phosphorus-based flame retardant on the flame retardancy of the epoxy resins, Polym. Degrad. Stabil. 109 (2014) 209–217.
[14] Xiaodong Qian, Lei Song, Yuan Hu, Richard KK. Yuen, Lijuan Chen, Yuqiang Guo, Ningning Hong, Saihua Jiang, Combustion and thermal degradation mechanism of a novel intumescent flame retardant for epoxy acrylate containing phosphorus and nitrogen, Ind. Eng. Chem. Res. 50 (4) (2011) 1881–1892.
[15] Zhenzhong Sun, Yanbei Hou, Yuan Hu, Weizhao Hu, Effect of additive phosphorusnitrogen containing flame retardant on char formation and flame retardancy of epoxy resin, Mater. Chem. Phys. 214 (2018) 154–164.
[16] Heeal Horacek, R. Grabner, Advantages of flame retardants based on nitrogen compounds, Polym. Degrad. Stabil. 54 (2–3) (1996) 205–215.
[17] Alexander B. Morgan, Non-Halogenated flame-retardant Handbook, John Wiley & Sons, 2021.
[18] Takashi Kashiwagi, Jeffrey W. Gilman, Silicon-based flame retardants. Flame Retardancy of Polymeric Materials, Marcel Dekker, New York, NY, 2000, pp. 353–389.
[19] Ging-Ho Hsiue, Wu-Jing Wang, Feng-Chih ChangSupSup, Synthesis, characterization, thermal and flame-retardant properties of silicon-based epoxy resins, J. Appl. Polym. Sci. 73 (7) (1999) 1231–1238.
[20] Baljinder K. Kandola, A Richard Horrocks, Peter Myler, Dana Blair, New developments in flame retardancy of glass-reinforced epoxy composites, J. Appl. Polym. Sci. 88 (10) (2003) 2511–2521.
[21] Hao Yongsheng, Fuchun Liu, Hongwei Shi, Enhou Han, Zhenyu Wang, The influence of ultra-fine glass fibers on the mechanical and anticorrosion properties of epoxy coatings, Prog. Org. Coating 71 (2) (2011) 188–197.
[22] Jamal Y. Sheikh-Ahmad, Machining of Polymer Composites, vol.387355391, Springer, 2009.
[23] K Mallick Pankar, Fiber-Reinforced Composites: Materials, Manufacturing, and Design, CRC press, 2007.
[24] T.P. Sathishkumar, S. Satheeshkumar, Jesuarockiam Naveen, Glass fiber-reinforced polymer composites-a review, J. Reinforc. Plast. Compos. 33 (13) (2014) 1258–1275.
[25] Xin Wang, Lei Song, Wiwat Pornwannchai, Yuan Hu, Baljinder Kandola, The effect of graphene presence in flame retarded epoxy resin matrix on the mechanical and flammability properties of glass fiber-reinforced composites, Compos. Appl. Sci. Manuf. 53 (2013) 88–96.
[26] WK Patrick Lim, M. Mariatti, W.S. Chow, K.T. Mar, Effect of intumescent ammonium polyphosphate (app) and melamine cyanurate (mc) on the properties of epoxy/glass fiber composites, Compos. B Eng. 43 (2) (2012) 124–128.
[27] D. Matykiewicz, B. Przybyszewski, R. Stanik, A. Czulak, Modification of glass reinforced epoxy composites by ammonium polyphosphate (app) and melamine polyphosphate (pna) during the resin powder molding process, Compos. B Eng. 108 (2017) 224–231.
[28] Q. Jiang, H. Zhang, D. Rusakov, N. Yousefi, A. Bismarck, Additive manufactured carbon nanotube/epoxy nanocomposites for heavy-duty applications, ACS Appl. Polym. Mater. 3 (1) (2020) 93–97.
[29] N. Yousefi, A.D. Evans, L.T. Harper, H.A. Maples, T. James, A. Bismarck, Solid epoxy resin systems for automated composite manufacturing, Compos. Appl. Sci. Manuf. 142 (2021) 106205.
[30] Christophe Floreani, Colin Robert, Parvez Alam, Peter Davies, Conchúr M.Ó Brádaigh, Mixed-mode interlaminar fracture toughness of glass and carbon fibre powder epoxy composites—for design of wind and tidal turbine blades, Materials 14 (9) (2021) 2103.
[31] Charles E. Harris, James H. Starnes Jr., Mark J. Shuart, Design and manufacturing of aerospace composite structures, state-of-the-art assessment, J. Aircraft 39 (4) (2002) 545–560.
[32] Emadelddin Hassan, Iasonas Zekos, Philip Jansson, Toa Pecur, Christophe Floreani, Colin Robert, Conchúr M.Ó Brádaigh, Margaret M. Stack, Erosion mapping of through thickness toughened powder epoxy gradient glass-fiber-reinforced polymer (gfrp) plates for tidal turbine blades, Lubricants 9 (3) (2021) 22.
[33] Steven M. Kurtz, Synthesis and processing of peek for surgical implants, in: PEEK Biomaterials Handbook, Elsevier, 2012, pp. 9–22.
[34] J.J. Murray, E.J. Pappa, Dimitrios Mamalis, Gearoid Breathnach, Adrian Doyle, Tomas Flanagan, Sandro Di Noi, C.M.O. Brádaigh, Characterisation of carbon fibre reinforced powder epoxy composites for wind energy blades, in: Proc. 18th Eur. Conf. Compos. Mater., Athens, Greece vol. 3, 2018.
[35] C. Robert, D. Mamalis, P. Alam, A.D. Lafferty, C.Ó Cadhain, G. Breathnach, E. D. McCarthy, C.M.Ó Brádaigh, Powder epoxy based ud-cfrp manufacturing routes for turbine blade application, in: SAMPE 2018, 2018.
[36] C. Robert, T. Pecur, E.D. McCarthy, C. Brádaigh, Tidal Turbine Blade Composites Using Basalt Fibre Reinforced Powder Epoxy, Barton, Australia, 2019, p. 3687. Engineers Australia.
[37] Colin Robert, Toa Pecur, James M. Maguire, Austin D. Lafferty, Edward D. McCarthy, Conchúr M.Ó Brádaigh, A novel powder-epoxy towpregging line for wind and tidal turbine blades, Compos. B Eng. 203 (2020) 108443.
[38] T.A. vd Misev, R. Van der Linde, Powder coatings technology: new developments at the turn of the century, Prog. Org. Coating 34 (1–4) (1998) 160–168.
[39] James M. Maguire, Kapileswar Nayak, Conchúr M.Ó Brádaigh, Characterisation of epoxy powders for processing thick-section composite structures, Mater. Des. 139 (2018) 112–121.
[40] C. Liu, T. Chen, C.H. Yuan, C.F. Song, Y. Chang, G.R. Chen, Y.T. Xu, L.Z. Dai, Modification of epoxy resin through the self-assembly of a surfactant-like multi-element flame retardant, J. Mater. Chem. A 4 (9) (2016) 3462–3470.
[41] Honghui Liao, Yuansen Liu, Jun Jiang, Yuan Liu, Wang Qi, Flame-retardant, glass fabric-reinforced epoxy resin laminates fabricated through a gradient distribution mode, J. Appl. Polym. Sci. 134 (2) (2017).
[42] A. Lucherini, C. Maluk, Intumescent coatings used for the fire-safe design of steel structures: a review, J. Constr. Steel Res. 162 (2019) 105712.
[43] A. Lucherini, L. Giuliani, G. Jomaas, Experimental study of the performance of intumescent coatings exposed to standard and non-standard fire conditions, Fire Saf. J. 95 (2018) 42–50.
[44] Weijie Li, Haiming Huang, Xiaoliang Xu, A coupled thermal/fluid/chemical/ablation method on surface ablation of charring composites, Int. J. Heat Mass Tran. 109 (2017) 725–736, 26-28 - 26-28.
[45] D. Morrisset, R.M. Hadden, A.I. Bartlett, A. Law, R. Emberley, Time dependent contribution of char oxidation and flame heat feedback on the mass loss rate of timber, Fire Saf. J. 120 (2021) 103058.

[46] M.J. Spearpoint, J.G. Quintiere, Predicting the burning of wood using an integral model, Combust. Flame 123 (3) (2000) 308–325.
[47] Mahdis Hesami, Rouhollah Bagheri, Mahmood Masoomi, Combination effects of carbon nanotubes, mmt and phosphorus flame retardant on fire and thermal resistance of fiber-reinforced epoxy composites, Iran. Polym. J. 23 (2014) 469–476.
[48] B. Shivamurthy, Gibin George, K Udaya Bhat, S. Anandhan, Influence of nano-aluminum hydroxide on tribological, mechanical and flammability properties of e-glass fabric/epoxy multi-layered laminates, KGK - Kautsch. Gummi Kunstst. 67 (6) (2014) 22–31.
[49] Mohammad Rajaei, De-Yi Wang, Debes Bhattacharyya, Combined effects of ammonium polyphosphate and talc on the fire and mechanical properties of epoxy/glass fabric composites, Compos. B Eng. 113 (2017) 381–390.
[50] Neeraj Mandlekar, Aurélie Cayla, François Rault, Stéphane Giraud, Fabine Salaün, Giulio Malucelli, Jin-Ping Guan, An overview on the use of lignin and its derivatives in fire retardant polymer systems, Lignin-Trends and Applications 9 (2018) 207–231.
[51] Henri Vahabi, Fouad Laoutid, Mehrshad Mehrpouya, Mohammad Reza Saeb, Philippe Dubois, Flame retardant polymer materials: an update and the future for 3d printing developments, Mater. Sci. Eng. R Rep. 144 (2021) 100604.
[52] Henri Vahabi, Fouad Laoutid, Mehrshad Mehrpouya, Mohammad Reza Saeb, Philippe Dubois, Flame retardant polymer materials: an update and the future for 3d printing developments, Mater. Sci. Eng. R Rep. 144 (2021) 100604.
[53] Kunal Wazarkar, Mukesh Kathalewar, Anagha Sabnis, Reactive modification of thermoplastic and thermoset polymers using flame retardants: an overview, Polym.-Plast. Technol. Eng. 55 (1) (2016) 71–91.
[54] Jun Jiang, Yanbo Cheng, Yuan Liu, Wang Qi, Yueshan He, Biwu Wang, Intergrowth charring for flame-retardant glass fabric-reinforced epoxy resin composites, J. Mater. Chem. A 3 (8) (2015) 4284–4290.
[55] Ruiqing Shen, Yufeng Quan, Qingsheng Wang, Thermal stability and flame retardancy of epoxy/synthetic fiber composites, in: Handbook of Epoxy/Fiber Composites, Springer, 2022, pp. 193–227.
[56] Quanyi Liu, Donghui Wang, Zekun Li, Zhifa Li, Xiaoliang Peng, Chuanbang Liu, Yu Zhang, Penglun Zheng, Recent developments in the flame-retardant system of epoxy resin, Materials 13 (9) (2020) 2145.
[57] Wei Jiang, Fan-Long Jin, Soo-Jin Park, Synthesis of a novel phosphorus-nitrogen containing intumescent flame retardant and its application to fabrics, J. Ind. Eng. Chem. 27 (2015) 40–43.
[58] Maria M. Velencoso, Alexander Battig, Jens C. Markwart, Bernhard Schartel, Frederik R. Wurm, Molecular firefighting—how modern phosphorus chemistry can help solve the challenge of flame retardancy, Angew. Chem. Int. Ed. 57 (33) (2018) 10450–10467.
[59] Pengju Liu, Wenhua Chen, Yuan Liu, Shibing Bai, Wang Qi, Thermal melt processing to prepare halogen-free flame-retardant poly (vinyl alcohol), Polym. Degrad. Stabil. 109 (2014) 261–269.
[60] T. Neumeyer, G. Bonotto, J. Kraemer, V. Altstaedt, M. Doering, Fire behaviour and mechanical properties of an epoxy hot-melt resin for aircraft interiors, Compos. Interfaces 20 (6) (2013) 443–455.
[61] Apollo Scientific Ltd. SAFETY DATA SHEET - 9,10-DIHYDRO-9-OXA-10-PHOSPHAPHENANTHRENE 10-OXIDE, 04 2019. Rev. vol. 2.
[62] V. Babrauskas, The Cone Calorimeter, SFPE handbook of fire protection engineering, 2016, pp. 952–980.
[63] B. Schartel, T.R. Hull, Development of fire-retarded materials—interpretation of cone calorimeter data, Fire Mater.: Int. J. 31 (5) (2007) 327–354.
[64] M.L. Janssens, Measuring rate of heat release by oxygen consumption, Fire Technol. 27 (1991) 234–249.
[65] Lijun Qian, Yong Qiu, Nan Sun, Menglan Xu, Guozhi Xu, Fei Xin, Yajun Chen, Pyrolysis route of a novel flame retardant constructed by phosphaphenanthrene and triazine-trione groups and its flame-retardant effect on epoxy resin, Polym. Degrad. Stabil. 107 (2014) 98–105.
[66] Siqi Huo, Jun Wang, Shuang Yang, Chuan Li, Xiaolei Wang, Haopeng Cai, Synthesis of a dopo-containing imidazole curing agent and its application in reactive flame retarded epoxy resin, Polym. Degrad. Stabil. 159 (2019) 79–89.
[67] Y. Yang, Q. Zhang, Y. Hao, X. Lan, L. Haurie, D. Zheng, G. Huang, Preparation of a cyclotriphosphazene microsphere bearing a phosphaphenanthrene structure towards fire-safety and mechanical enhancement for epoxy and its aramid fiber composite, Mater. Adv. 5 (7) (2024) 2860–2871.
[68] P.M. Hergenrother, C.M. Thompson, J.G. Smith, J.W. Connell, J.A. Hinkley, Flammability of Epoxy Resins Containing Phosphorus, 2005. No. PB2006-102392).